Experimental Analysis and Orthotropic Hyperelastic Modelling Of Textile Woven Fabric

R. Zouari[1], S. Ben Amar[2], A. Dogui[1]

[1]Mechanical Engineering Laboratory, ENIM, University of Monastir, Monastir, TUNISIA

[2]Energy and Thermal Systems Laboratory, ENIM, University of Monastir, Monastir, TUNISIA

Correspondence to:
Rym Zouari, email: zouarirym@yahoo.fr

ABSTRACT

This paper presents an experimental study and hyperelastic modelling of orthotropic mechanical behavior of woven textile fabric. The strain energy function of the hyperelastic model is a combination of the warp extension, weft extension, and shear angle between warp and weft directions. The experimental and fitting analysis of the anisotropy is realized using off-axis tensile tests for five textile woven fabrics. Orthotropic hyperelastic modelling highlights the anisotropy tensile property of textile woven fabric compared to orthotropic linear elastic modelling. Particular attention is given to the influence of weave structure on fabric anisotropy.

Keywords: Textile woven fabric, Off-axis tensile test, Anisotropy, Hyperelastic modelling.

INTRODUCTION

Several research studies have considered the complex anisotropic behavior of textile woven fabric. Most of them [1, 2, 5] focused on the linear uniaxial tensile Stress/Strain behavior along the warp, weft, and 45° oriented fabric directions.

Woven fabric is highly anisotropic, as it exhibits different mechanical properties for different directions. An experimental approach is applied in order to evaluate and characterize this anisotropy. Off-axis tensile testing is generally employed for highly anisotropic composite materials [6, 8]. This test is a tensile test along a direction other than warp and weft. Ning [7] studied the influence of varying directions of off-axis tensile tests over the tensile and shear strengths before buckling.

A linear elastic orthotropic model has already been developed by the authors [9], and its parameter identified for a particular zone of the woven fabric tensile curve. An analysis of the anisotropy has also been presented. The continuous domain approach gives satisfactory results for elastic linear orthotropic modelling. However, it is considered as a simplified modelling in a limited zone of load, if the strain rate remains constant.

An orthotropic hyperelastic model is developed for a continuum material equivalent to the woven fabric [4, 10]. The nonlinear relationship between stress and strain is then highlighted.

In this paper, off-axis tensile tests are carried out on five fabrics. Fitting results obtained by Model 1 (linear orthotropic elastic model) and Model 2 (orthotropic hyperelastic model) are compared using an anisotropic degree of elastic modulus for fabrics 1 and 2.

Particular attention is given to the effect of weave structure on the anisotropic behavior for fabric 3, 4 and 5.

MATERIALS AND METHODS

Description of Off-Axis Tensile Test

Off-axis tensile tests were carried out on five fabrics whose principal characteristics are as shown in *Table I*. Fabrics 1 and 2 are unbalanced and fabrics 3, 4, and 5 which have the same yarn in the warp and the weft direction are balanced.

The specimen test has a useful zone of 200 mm length x 50 mm width between the grips (*Figure 1*). The specimen was cut in seven directions forming an angle ψ with the warp direction (0°, 15°, 30°, 45°, 60°, 75° and 90°). The form of specimen is illustrated by the *Figure 1*. Tests were carried out with articulated jaws designed to allow a free rotation along the specimen's normal direction. Off-axis tensile tests were repeated five times for all directions. The strain rate was 100 mm/min.

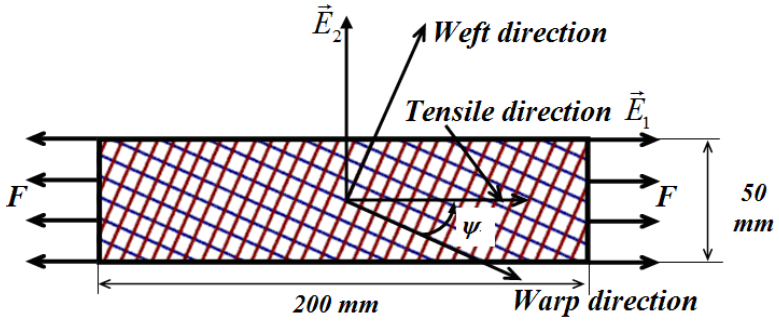

FIGURE 1. Off-axes tensile test.

TABLE I. Description of fabrics.

		Warp direction			Weft direction			Fabric areal density (g/m2)	Thickness fabric (mm)
		Yarn fibers	Yarn linear density (Tex)	Sett (Yarn/cm)	Yarn fibers	Yarn linear density (Tex)	Sett (Yarn/cm)		
Fabric1	Twill 3	Cotton	19.4	39	Cotton	42	24	195	0.5
Fabric2	Plain	Polyester Polyamide	18 17.5	17	Polyester Cotton	50 33	16	110	0.39
Fabric3	Plain	52%Polyester 48%Coton	27,8	24	52%Polyester 48%Coton	27,8	26	182	0.41
Fabric4	Twill 4	52%Polyester 48%Coton	27,8	24	52%Polyester 48%Coton	27,8	24	178	0.51
Fabric5	Satin 4	52%Polyester 48%Coton	27,8	24	52%Polyester 48%Coton	27,8	24	175	0.5

Anisotropic Behavior

For each direction, we were interested in the curve near to the average of the five results obtained. Off-axis tensile curves analysed were load-extension curves before buckling for all fabrics.

Fabric tensile behavior is nonlinear; it's illustrated by *Figures 2, 3, 4, 5 and 6* respectively for fabrics 1, 2, 3, 4 and 5.

Tensile test curves start with a nonlinear zone followed by a linear one. The determining parameters in the wide nonlinear zone [3] are the fabric structure, crimp, the slip between warp and weft yarns, and the initial yarn undulation.

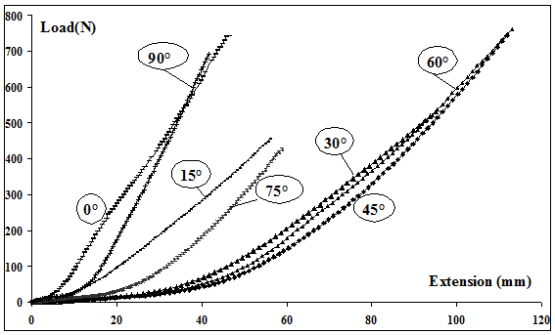

FIGURE 2. Load-extension curves before buckling, fabric 1.

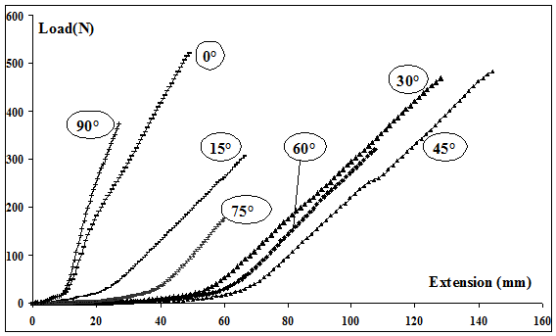

FIGURE 3. Load-extension curves before buckling, fabric 2.

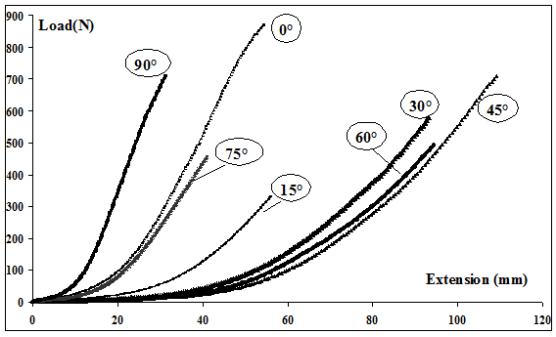

FIGURE 4. Load-extension curves before buckling, fabric 3.

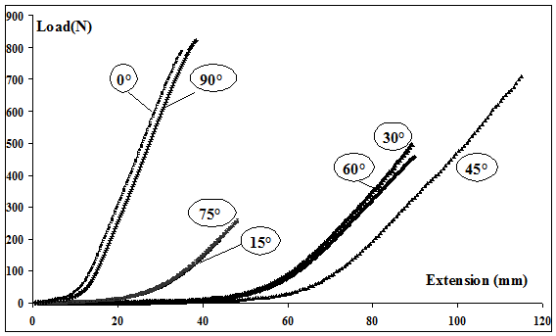

FIGURE 5. Load-extension curves before buckling, fabric 4.

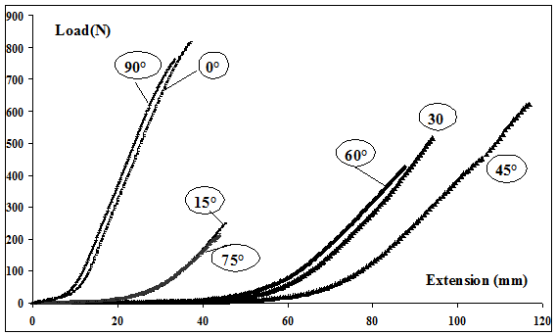

FIGURE 6: Load-extension curves before buckling, fabric 5.

COMPARISON BETWEEN MODEL 1 AND MODEL 2

Woven fabric mechanical behavior is nonlinear but we sought to associate analytic models [9] to the linear zone of the load-extension curve in order to characterize quantitatively the anisotropy. *Figure 7* presents the experimental and linear zone of the load-extension curves along the weft direction for fabric1.

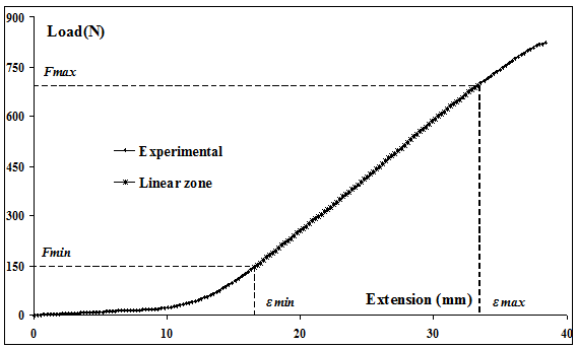

FIGURE 7. Experimental and linear zone load-extension curves, weft direction, fabric 1.

Orthotropic linear elastic model: Model 1

An off-axis tensile test of the orthotropic linear elastic material is defined [9] by:

$$\varepsilon \equiv C(\psi)\,\mathrm{P};\ C(\psi) = C_0 \cos^4\psi + C_{90}\sin^4\psi + (C_{45} - \frac{1}{4}(C_0 + C_{90}))\sin^2 2\psi \quad (1)$$

where:

C (mm^2/N) is the elastic modulus

The first Piola- Kirchhoff stress P(N /mm^2) =F/S_0

The deformation ε=$\Delta L/L_0$

L_0 (mm) is the initial length, ΔL (mm) is the extension, F (N) is the load, and S_0 is the initial section; the initial width multiplied by the initial thickness.

Orthotropic Hyperelastic Model: Model 2

Woven textile fabric is considered as a continuous medium having two privileged material directions; warp and weft; defined by the two unit tensors $\boldsymbol{g}_1 = \vec{E}_1 \otimes \vec{E}_1$ and $\boldsymbol{g}_2 = \vec{E}_2 \otimes \vec{E}_2$.

Where $\vec{E}_1$ and $\vec{E}_2$ are units vectors (*Figure 1*).

In Lagrangian formulation, the hyperelastic behavior is completely defined by the strain energy function $W(\boldsymbol{E})$ depending on Green-Lagrange strain tensor $\boldsymbol{E}$.

The second Piola Kirchhoff stress tensor $\boldsymbol{S}$ derives then from this energy: $\boldsymbol{S} = \partial W/\partial \boldsymbol{E}$. The physical behavior is completely defined by the choice of $W(\boldsymbol{E})$.

The developed strain energy function is a quadratic function of invariants; it's a function of the warp and weft deformation and the shear angle between warp and weft directions [4, 10]. The orthotropic hyperelastic continuum model will be thus linear between $\boldsymbol{S}$ and $\boldsymbol{E}$. We are more particularly interested to plane solicitations and the only coupling permitted is between slip and extension along the warp and weft directions. The strain energy function W is defined as follows:

$$W = \tfrac{1}{2} k_1 I_1^2 + \tfrac{1}{2} k_2 I_2^2 + k_{12} I_1 I_2 + k_3 I_{12}^2 \quad (2)$$

Where k_1 and k_2 are the tensile rigidity along the warp and weft yarns, k_{12} is the interaction between them, k_3 is the shearing rigidity. Principals invariants I_i and I_{12} are defined by Eq. (3) [4, 10].

$$I_i = \boldsymbol{g_i}:\boldsymbol{E}; \quad I_{12} = (\boldsymbol{g_1}\boldsymbol{E}:\boldsymbol{E}\,\boldsymbol{g_2}) \quad (3)$$

The second Piola–Kirchoff stress tensor $\boldsymbol{S}$ is written as:

$$\boldsymbol{S} = (k_1 I_1 + k_{12} I_2)\,\boldsymbol{g_1} + (k_2 I_2 + k_{12} I_1)\,\boldsymbol{g_2} + k_3(\boldsymbol{g_1}\boldsymbol{E}\boldsymbol{g_2} + \boldsymbol{g_2}\boldsymbol{E}\boldsymbol{g_1}) \quad (4)$$

The response of the model to the off-axis tensile test can be summarised as follows:

$$E = C(\psi) S \quad (5)$$

Where E is the Green–Lagrange deformation and S(N /mm^2) is second Piola–Kirchoff uniaxial stress defined respectively by :

$$E = \tfrac{1}{2}((\varepsilon+1)^2 - 1) \text{ and } S = P/((\varepsilon+1)) \quad (6)$$

Elastic modulus is defined by Eq. (1) with:

$$C_0 = \frac{k_2}{k_1 k_2 - k_{12}^2}$$
$$C_{90} = \frac{k_1}{k_1 k_2 - k_{12}^2} \quad (7)$$
$$C_{45} = \frac{1}{2}\frac{1}{k_3} - \frac{1}{4}\frac{2k_{12} + k_1 + k_2}{k_1 k_2 - k_{12}^2}$$

Data Analysis

In this part, we are particularly interested in the variation of elastic modulus for models 1 and 2; C is identified for the same linear zone of load-extension curve of 7 directions for fabrics 1 and 2 for both models.

Elastic modului, C_0, C_{90} and C_{45} are identified by fitting the function C with the experimental values of both models. *Figure 8* illustrates the experimental and fitting curves for model 1 and 2 along the weft direction for fabric 1.

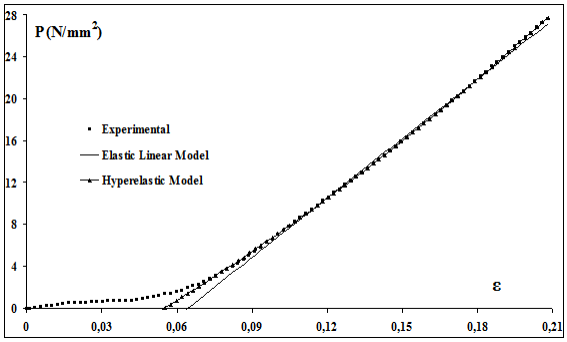

FIGURE 8. Experimental and fitting curves, model 1 and 2, weft direction, fabric 1.

Table II presents fitting elastic modulus for models 1 and 2. *Figure 9* and *Figure 10* present the results of this identification as well as the comparison between the fitting and the experimental values for both models respectively for the fabrics 1 and 2.

The analytical average elastic modulus $\bar{C}$, the discrete average elastic modulus $\bar{C}_d$ and the anisotropy degree of elastic modulus C_a are defined respectively by Eq. (8), Eq. (9) and Eq. (10). These grandeurs are calculated to view the degree of anisotropy of models 1 and 2.

$$\bar{C} = \frac{1}{\pi/2}\int_0^{\pi/2} C(\psi)d\psi = \frac{C_0 + C_{90} + 2C_{45}}{4} \quad (8)$$

$$\bar{C}_d = \frac{1}{7}\sum_{0}^{7} C_i(\psi) \quad (9)$$

$$C_a = \frac{2C_{45} - (C_0 + C_{90})}{2\bar{C}} \quad (10)$$

The analytic average elastic modulus and the anisotropy degree of elastic modulus are higher for model 2 than model 1, shown in *Table III*.

Anisotropy indicators C_a and coefficient of variation show that model 2 revealed more the anisotropic tensile property of textile woven fabric than model 1.

TABLE II. Fitting elastic modulus for model 1 and 2.

ψ (°C)	C (mm²/N): Fabric 1		C (mm²/N): Fabric 2	
	Model 1	Model 2	Model 1	Model 2
0	0.0071	0.0103	0.0082	0.0127
15	0.0090	0.0195	0.0147	0.0303
30	0.0126	0.0244	0.0158	0.0408
45	0.0141	0.0254	0.0164	0.0430
60	0.0117	0.0230	0.0150	0.0371
75	0.0074	0.0171	0.0127	0.0239
90	0.0053	0.0075	0.0052	0.0053

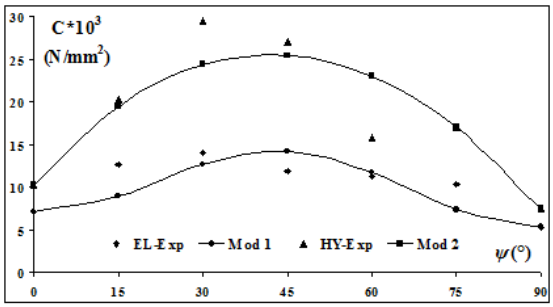

FIGURE 9. Experimental and analytic elastic modulus for model 1 and 2, fabric 1.

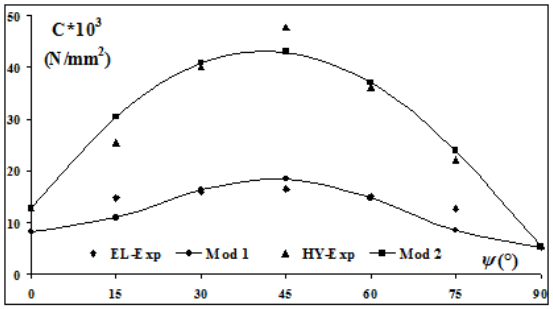

FIGURE 10. Experimental and analytic elastic modulus for model 1 and 2, fabric 2.

TABLE III. Anisotropy degree of elastic modulus, fabric 1 and 2.

		Discrete average elastic modulus	Analytic average elastic modulus	Anisotropy degree of elastic modulus	Coefficient of Variation
		$\bar{C}_d$ (mm²/N)	$\bar{C}$ (mm²/N)	C_a (mm²/N)	(C max- C min)/ $\bar{C}$
Fabric 1	Model 1	0.0096	0.0102	0.78	0.87
	Model 2	0.0182	0.0172	0.96	1.04
Fabric 2	Model 1	0.0125	0.0125	0.94	1.05
	Model 2	0.0276	0.0260	1.30	1.45

WEAVE STRUCTURE EFFECT

In this part, we are only interested in model 2 responses for balanced fabrics 3, 4 and 5.

Experimental Results

Figures 11, 12 and 13 give S (E_1) curve before buckling for fabrics 3, 4 and 5. For fabric 3, behavior along the warp direction is different from weft direction, as well as for the directions oriented by 15° and 75° and along the direction oriented by 30° and 60°. This is due to the characteristic of plain weave: more interlacing points warp/weft for the same number of yarn, and the importance of warp crimp (12%) to weft crimp (5%); like warp and weft crimp for fabrics 4 and 5.

For fabrics 4 and 5, we have a similar behavior along the warp and weft direction, an analogous behavior along the direction oriented by 15° and 75° and along the direction oriented by 30° and 60°. The 45° oriented direction permits the higher elongation for the three fabrics.

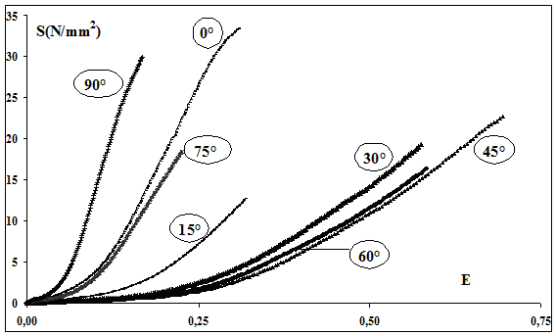

FIGURE 11. Experimental curve S (E_1), fabric 3.

Identification of Elastic Modulus

We have non-linear off-axis tensile curves S (E) for fabrics 3, 4, 5. But, we sought to associate model 2 for the linear zone of S (E) curve. Experimental elastic modulus is determinate for fabrics 3, 4 and 5 along the different directions solicited.

Identification of elastic modulus is obtained by fitting the function $C(\psi)$ given by Eq. (7) with the experimental values for the 7 directions for fabrics 3, 4 and 5.

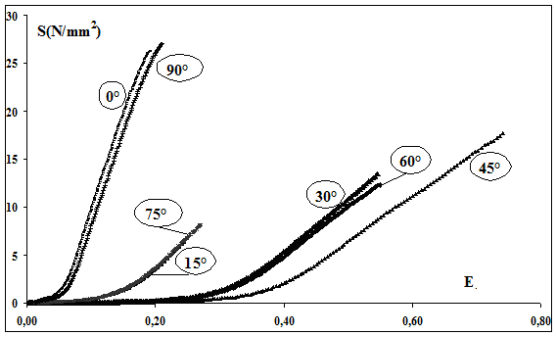

FIGURE 12. Experimental curve S (E_1), fabric 4.

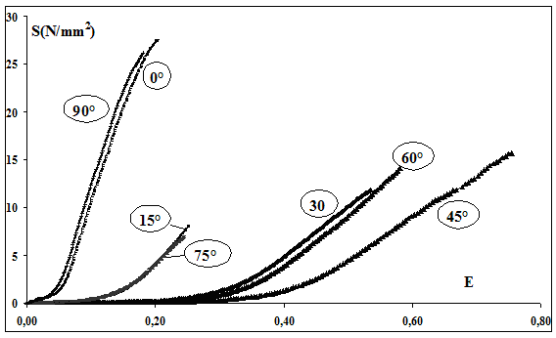

FIGURE 13. Experimental curve S (E_1), fabric 5.

RESULTS AND DISCUSSION

Elastic Modulus

Figure 14 shows experimental and fitted elastic modulus for fabrics 3, 4 and 5. We observe a similar experimental result in various directions for fabrics 4 and 5. We obtain different results along the 15°, 45° and 75° oriented directions for these fabrics. Only fabric 3 has a different result from warp direction compared to weft direction (*Table IV*), although we have a balanced fabric and the same warp and weft yarn property. This is due to the typical plain weave structure: the number of interlacing point is double those of twill and satin weave structures and the warp crimp to weft crimp is significantly different.

The variation of elastic modulus values is more evident for the fitted results than the experimental results. *Table IV* presents similar fitted results for fabrics 4 and 5.

Anisotropy is illustrated by the dependence of the elastic modulus on angle between solicited direction and the warp direction. In fact, *Table IV* shows different elastic modulus values for all directions.

The discrete average elastic modulus $\overline{C}_d$, the analytic average elastic modulus $\overline{C}$ and the anisotropy degree of elastic modulus C_a are lower for fabric 3 and similar for fabrics 4 and 5, as shown in *Table V*.

The coefficient of variation is more than that of C_a and the disparity is considerably more (21 %) than the C_a disparity for three fabrics.

So, anisotropy is more significant for fabric 5 followed by fabric 3 than fabric 4.

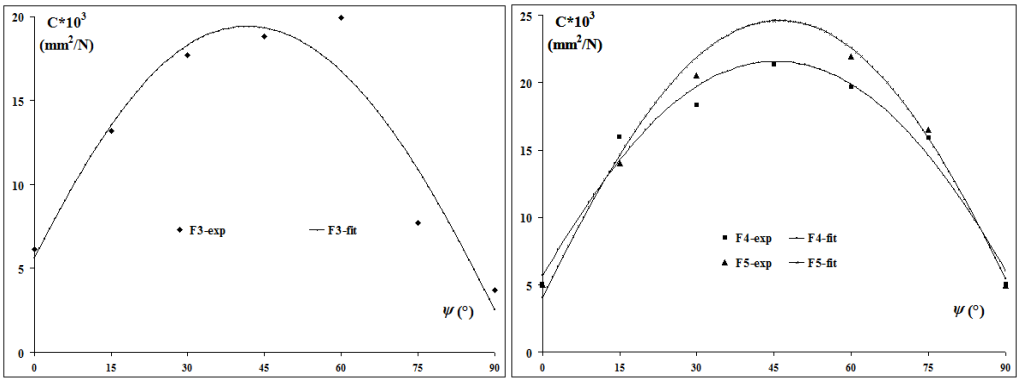

FIGURE 14. Experimental and fitted elastic modulus, fabric 3, 4 and 5.

TABLE IV. Experimental and fitted elastic modulus, fabric 3, 4 and 5.

ψ (°C)	C (mm²/N): Fabric 3		C (mm²/N): Fabric 4		C (mm²/N): Fabric 5	
	Experimental	Fitting	Experimental	Fitting	Experimental	Fitting
0	0.0062	0.0056	0.0050	0.0057	0.0050	0.0041
15	0.0132	0.0135	0.0160	0.0143	0.0128	0.0147
30	0.0177	0.0183	0.0184	0.0197	0.0178	0.0219
45	0.0178	0.0193	0.0214	0.0216	0.0226	0.0246
60	0.0199	0.0167	0.0197	0.0199	0.0191	0.0226
75	0.0077	0.0109	0.0160	0.0146	0.0144	0.0159
90	0.0037	0.0025	0.0051	0.0060	0.0048	0.0055

TABLE V. Anisotropy degree of elastic modulus, fabric 3, 4 and 5.

	Discrete average elastic modulus $\overline{C}_d$ (mm²/N)	Analytic average elastic modulus $\overline{C}$ (mm²/N)	Anisotropy degree of elastic modulus C_a (mm²/N)	Coefficient of Variation (C max- C min)/ $\overline{C}$
Fabric 3	0.0124	0.0117	1.30	1.44
Fabric 4	0.0146	0.0137	1.15	1.16
Fabric 5	0.0156	0.0147	1.35	1.40
Disparity (%) (Ymax-Ymin) /Ymoy	22	22	16	21

TABLE VI. Fitting rigidity material coefficient, fabric 3, 4 and 5 .

	k_1 (N/mm²)	k_2 (N/mm²)	k_3 (N/mm²)
Fabric 3	178	395	29
Fabric 4	176	165	29
Fabric 5	246	183	22

Rigidity Material Coefficient

Particular attention was given to the identification of the rigidity material model coefficients. Using only S (E) results cannot be used to estimate all the rigidity material coefficients. Using Eq. (1), we can identify only 3 independents coefficients then, we cannot identify the four coefficients k_i and k_{12}. But, assuming k_{12}=0 (neglecting the interaction between warp and weft yarns), the 3 coefficients k_i are related to the 3 coefficients C by:

$$C_0 = \frac{1}{k_1}$$
$$C_{90} = \frac{1}{k_2} \quad (11)$$
$$C_{45} = \frac{1}{2}\frac{1}{k_3} - \frac{1}{4}\frac{k_1 + k_2}{k_1 k_2}$$

We obtained the values illustrated in *Table VI*. We have an equivalent fitted rigidity material coefficient for fabrics 4 and 5 (similar results).

Plain fabric presents more rigidity along the warp direction than weft direction; tensile rigidity k_2 is greater than k_1. k_1 and k_2 are influenced by the distribution of yarn interlacing and the effect of the repetition of the motif on the weave structure in the fabric. Shearing k_3 rigidity of the woven fabric is further significant for fabric 3 followed by fabric 4 then fabric 5. Mechanical properties depend to woven fabric structure.

CONCLUSION

Off-axis tensile tests made on five fabrics and used to distinguish woven fabric anisotropy. An analysis of anisotropy of elastic modulus using an orthotropic linear elastic model and the orthotropic hyperelastic model is presented.

The experimental process revealed that woven fabric anisotropy depends on weave fabric structure and the loading direction. This influence is due to the influence of warp and weft yarn deformations, fabric structure, and yarn mechanical property.

It is verified for fabrics 1 and 2 that the orthotropic hyperelastic model better characterizes woven fabric anisotropic tensile property than the orthotropic linear elastic model.

Using the hyperelastic model, the fitted results are in good accord with the experimental ones.

REFERENCES

[1] Banerjee P.K., Swapna M., Thiyagarajan R. 2010. Effect of Sett and Construction on Uniaxial Tensile Properties of Woven Fabrics. *The Textile Research Journal*, 69, 866–875.

[2] Bassett R.J., Postle R. 1999. Experimental methods for measuring fabric mechanical properties: A review and analysis. *The Journal of Engineered Fibres and fabrics*, 5, 8–21.

[3] Boisse,P. Zouari,B., Dumont,F., Gasser,A. 2005. Assemblage des fibres par tissage: analyse et simulation du comportement mécanique. *Mécanique et industries*, 6, 65-74.

[4] Dridi S., Dogui A., Boisse P. 2011. Finite element analysis of bias extension test using an orthotropic hyperelastic continuum model for woven fabric, *The Journal of the Textile Institute*, 102, 781–789.

[5] Hu, J.L., Lo,W.M. 2002. Shear Properties of Woven Fabrics in Various Directions. *Textile Research Journal*, V72, pp.383-390

[6] Ng S.P., Ng R., Yu W. 2005. Bilinear approximation of anisotropic Stress-Strain properties of woven fabrics. *The Research Journal of Textile and Apparel*, 9, 1–15.

[7] Ning P., Yoon M.Y. 1996. Structural anisotropy, failure criterion and shear strength of woven fabrics. *The Textile Research Journal*, 66, 238–244.

[8] Zheng J., Takatera M., Shigeru I., Shimizu Y. 2008, Measuring Technology of the Anisotropic Tensile Properties of Woven Fabrics. *The Textile Research Journal*, 78, 1116–1123.

[9] Zouari R., Ben Amar S. Dogui A. 2010. Experimental and numerical analyses of fabric off-axes tensile test, *The Journal of the Textile Institute*, 101, 58–68.

[10] Zouari R., Ben Amar S. Dridi S., Dogui A. 2008. An orthotropic hyperelastic continuum model for woven fabric: Application to out-axis tensile and shearing, *4th International Conference on Advances in Mechanical Engineering and Mechanics*, Sousse, Tunisia.

AUTHORS' ADDRESSES

Rym Zouari, PhD
Abdelwaheb Dogui
Mechanical Engineering Laboratory
ENIM, University of Monastir,
Avenue Ibn El Jassar
Monastir, Tunisia 5019
TUNISIA

Sami Ben Amar, PhD
Energy and Thermal Systems Laboratory
ENIM, University of Monastir,
Avenue Ibn El Jassar
Monastir, Tunisia 5019
TUNISIA